Supplementary Information

Towards the Selectivity and Energetics of anti-Bredt Olefins - A Density Functional Theory Approach

Pritam Chakraborty[†], Jannat Alam[†], Bibitha Poulose, Shyama Ramakrishnan and Padmesh Anjukandi*

Department of Chemistry, Indian Institute of Technology Palakkad,

Kerala, India.

Contents

1 Computational Methods

Benchmarking:

To determine the most suitable method for these calculations, we conducted benchmarking using various functionals and basis sets. The analysis is focused on the parameters like twist angle, pyramidalization angle, bond length, and bond order of ABO (Fig 2 C) that were specified in previous studies [1] and also activation energy comparison between Pentacoordinated siliconate complex (PCC) (Fig 2B) and TS-1 (Fig 2, TS-1). The table below presents a comparison of the results obtained with different functionals and basis sets.

Table S1: Benchmarking of the parameters with different functionals

Method	Twist angle	Pyramidalized angle	Bond length (C_1–C_2)	Bond order (C_1–C_2)	PCC Energy (kcal/mol)	TS-1 Energy (kcal/mol)	$\Delta G_{TS\text{-}1} - \Delta G_{PCC}$	Computational Cost
wB97XD/def2-TZVP (paper)	35.5	C_1: 20.1 C_2: 11.6	1.35 Å	1.86	–	–	–	–
BP86/def2-TZVPD/D3BJ	35.58	C_1: 35.42 C_2: 13.80	1.36 Å	1.89	-1094255.97356	-1094252.20997	3.77	2 hr 36 min
B3LYP/def2-TZVPD/D3BJ	35.43	C_1: 32.01 C_2: 13.87	1.35 Å	1.92	-1093805.6605	-1093801.07844	4.58	11 hr 51 min
BP86/SVP/D3BJ	36.22	C_1: 34.65 C_2: 12.20	1.37 Å	1.89	-1093288.86924	−1093282.97692	5.89	20 min

The structural parameters, including twist angle, pyramidalization angle, bond length, and bond order, are in good agreement with values reported in previous studies across all functionals and basis sets. However, the calculated activation energies exhibit some variation. Specifically, the BP86/SVP [2, 3, 4] and B3LYP/def2-TZVPPD [5, 6] levels differ by about 1.31 kcal/mol. Considering both accuracy and efficiency, we chose the BP86/SVP level for our further calculations.

Initial structures were drawn using Gaussview and were optimised in ORCA 6.0 [7, 8] at the BP86/SVP/D3BJ [9] level of theory. Frequency calculations were performed to check all the stationary points in the potential energy surface to characterize them as transition state or minima. Chemcraft and VMD software [10] was used for visualization purposes.

2 Comparison of the parameters of both ABOs

Both isomers are capable of generating ABO; however, only one pathway is energetically feasible. iso-1 yields ABO-C, whereas iso-2 leads to ABO-F (Fig 2).

Table S2: Comparison of the calculated parameter values for the corresponding ABOs

ABOs	**ABO-C**	**ABO-F**
Twist angle	36.22°	55.5
Pyramidalized angle	C_1: 34.65 C_2: 12.20	C_1: 39.41 C_2: 29.75
Bond length (C_1-C_2)	1.37	1.40
Bond order	1.89	1.86

From the table it can be said that ABO-F is very unstable because of the high twist and pyramidalized angle.

3 Potential Energy Surface Scan

3.1 1D Potential Energy Surface Scan

A one-dimensional (1D) potential energy scan is a computational technique used to investigate how the potential energy of a molecule varies with respect to a single internal coordinate. The selected coordinate may correspond to a bond length, bond angle, or dihedral angle, depending on the chemical process of interest.

This method is particularly useful for examining the relationship between molecular structure and energy. By systematically varying one structural parameter, it becomes possible to identify energy minima (corresponding to stable conformations) and energy maxima (associated with transition states). To investigate the energetics and reaction pathway of iso-1 and iso-2, a one-dimensional scan was performed.

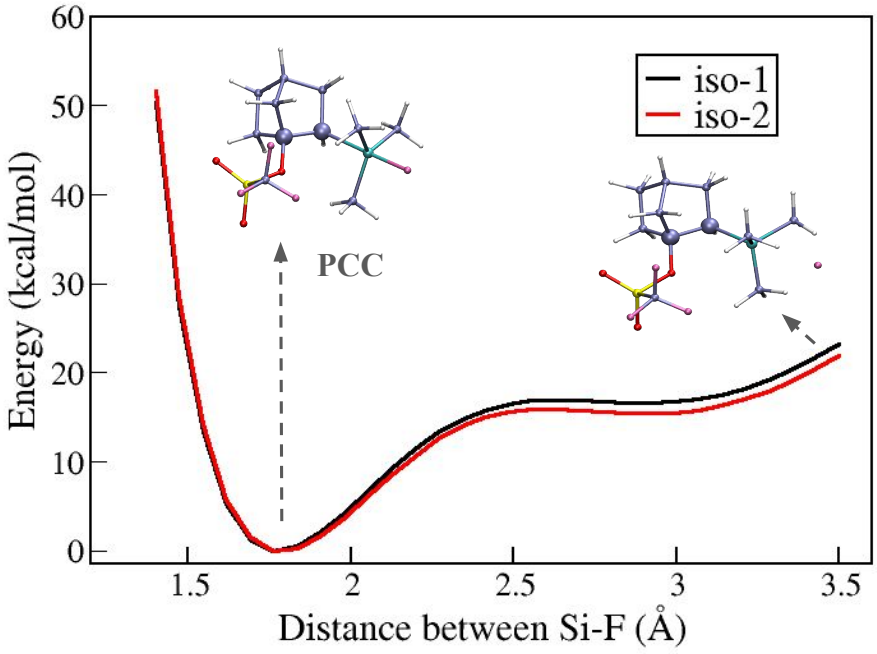

Figure S1: Potential energy surface scan depicting the approach of the fluoride ion toward the silicon atom of the TMS group, leading to the formation of a pentacoordinated siliconate complex (PCC) for iso-1 (black) and iso-2 (red).

Figure S1 shows the potential energy surface for the Si–F bond, mapped over a range from 3.5 Å to 1.4 Å. The black line represents precursor iso-1, while the red line corresponds to precursor iso-2. As the fluoride ion approaches the TMS group, it initially engages in dipole–dipole interactions with the methyl groups of TMS, eventually leading to the formation of an energetically stable pentacoordinated siliconate complex (shown in Fig 2B and Fig 2D). Notably, the formation of this pentacoordinated complex occurs without any energy barrier.

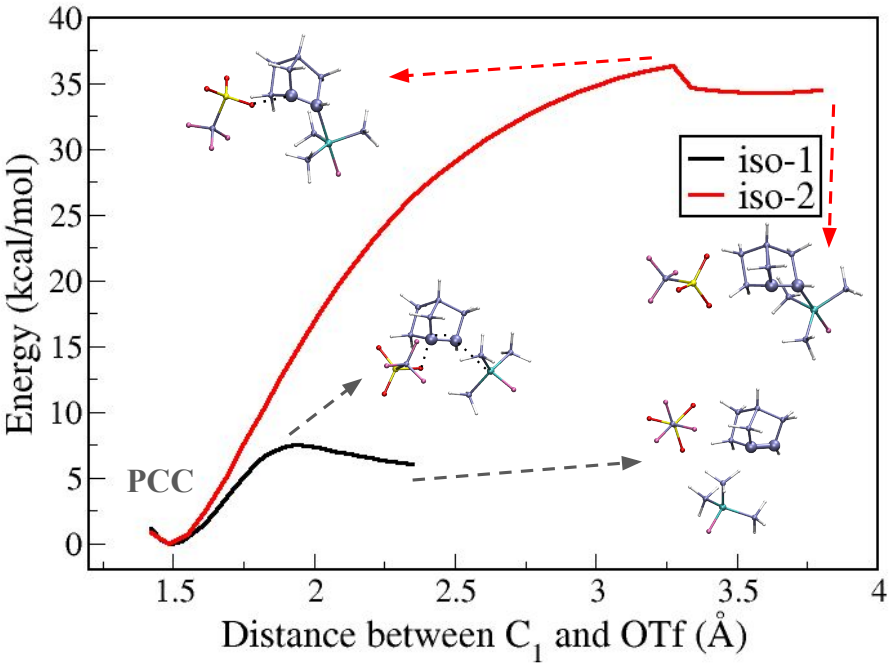

Figure S2: Potential energy surface scan illustrating the dissociation of the OTf group from the stable pentacoordinated siliconate complex for iso-1 (black) and iso-2 (red).

Figure S2 displays the potential energy surface for the C_1–OTf bond. The stable pentacoordinated siliconate complex (Fig 2B and Fig 2D) was first optimized and then subjected to a scan. For iso-1, the scan ranged from 1.42 Å to 2.5 Å, leading to the formation of the product (Fig 2C) via a transition state (Fig 2. TS-1), during which both the C_1– OTf and C_2–Si bonds simultaneously broke. In contrast, for iso-2, scanning the C_1– OTf bond up to 2.5 Å revealed no local minima or product. Extending the scan to 4 Å resulted in a product (Fig 2E) formed through a transition state (Fig 2. TS-2), where the C_1–OTf bond had broken and the OTf group departed, but the C–Si bond remained intact despite the cleavage of the C_1–OTf bond.

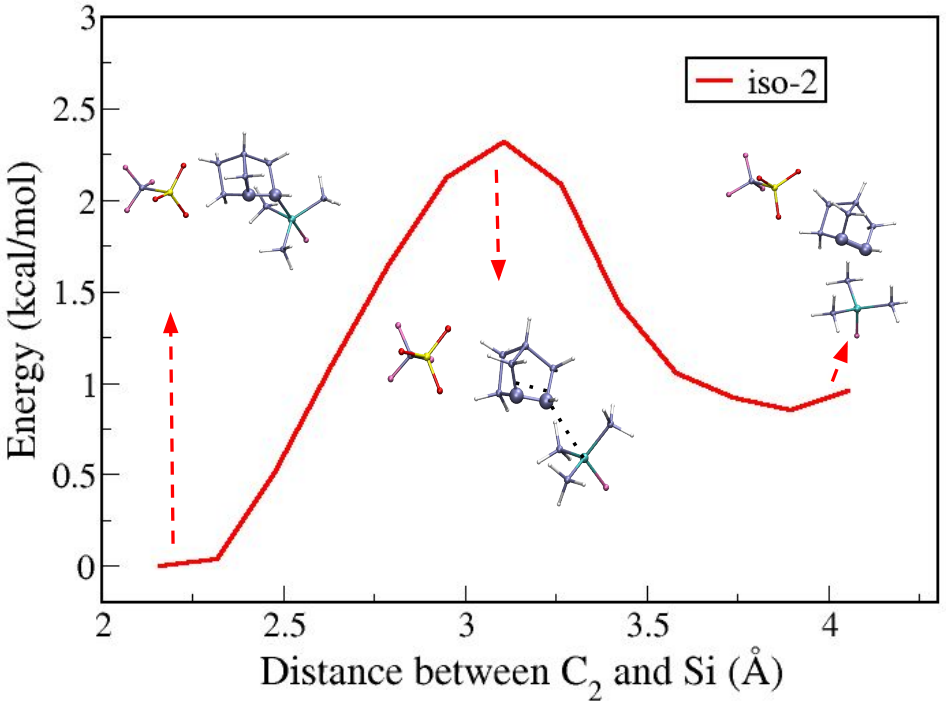

Figure S3: Potential energy surface scan for iso-2 illustrating the dissociation of the TMSF group.

Since iso-2 did not form a product during the C_1–OTf bond scan, an additional scan was performed starting from the last product obtained (Fig 2E), focusing on the C–Si bond over a range of 2 Å to 5 Å (Fig S3). This scan led to the formation of the product shown in Fig 2F through the transition state depicted in Fig 2 TS-3.

3.2 2D Potential Energy Surface Scan

A two-dimensional (2D) potential energy scan extends the concept of a 1D potential energy scan by simultaneously varying two internal coordinates. This generates a grid of energy values that can be represented either as a three-dimensional surface or as a contour map.

This method is particularly useful when the system's behavior depends on the interplay between two structural parameters. It enables the exploration of reaction pathways, conformational energy landscapes, and coupled motions that cannot be adequately described by a single-coordinate scan.

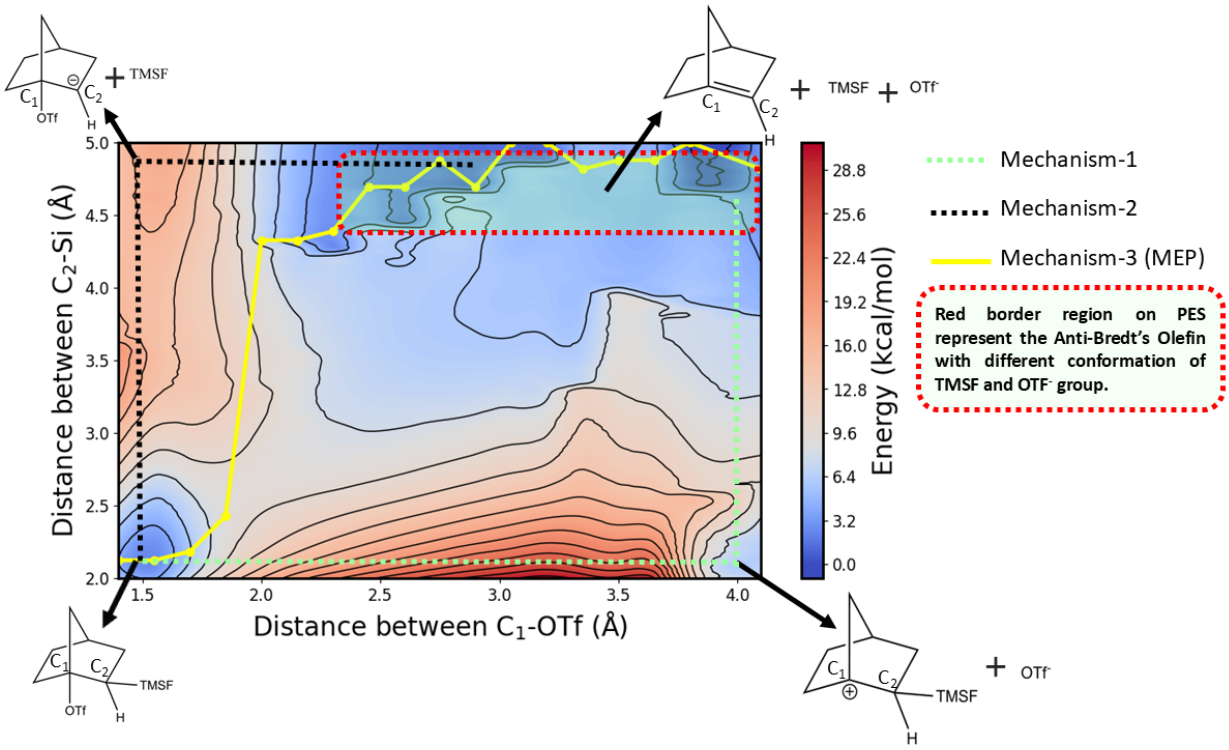

Figure S4: Two-dimensional Potential Energy Surface (PES) scan of iso-1. The yellow line denotes the Minimum Energy Path (MEP), whereas the green and black dotted lines correspond to alternative mechanistic path that may also facilitate the formation of the anti-Bredt olefin. The grid spacing is 0.15 Å along the x-axis and 0.06 Å along the y-axis.

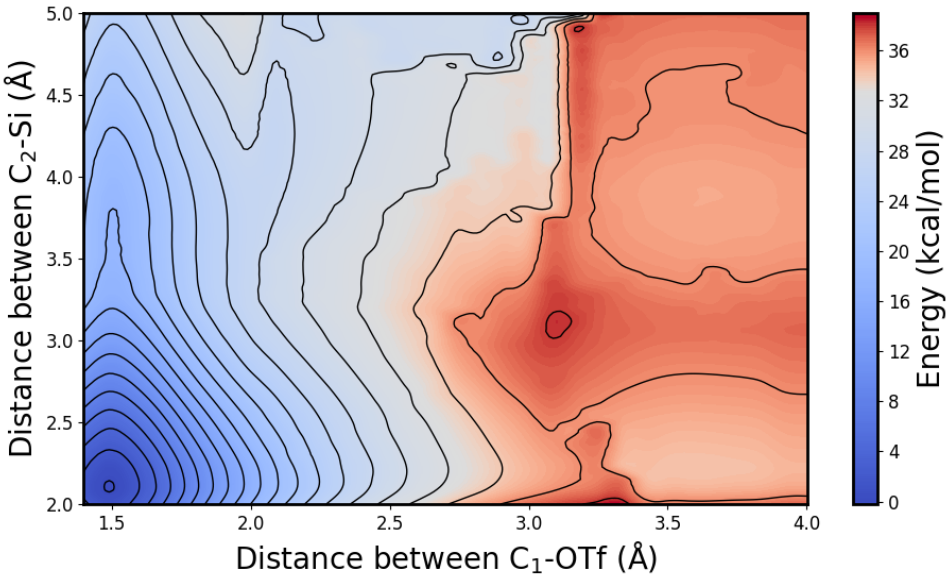

Figure S5: Two-dimensional Potential Energy Surface (PES) scan of iso-2. It can be observed that the formation of the product is not favorable, as the resulting anti-Bredt olefin is unstable. The grid spacing is 0.08 Å along x-axis and 0.07 Å along the y-axis.

4 Possible Mechanism of formation of anti-Bredt Olefin

From Figure S1, it is evident that the formation of the pentacoordinated siliconate complex (PCC) is highly feasible, occurring through an almost barrierless process for both isomers. Once a stable PCC is formed, it can proceed through three possible mechanistic pathways leading to the formation of the anti-Bredt olefin. These three possible mechanisms are discussed below:

4.1 Mechanism-1:

After the formation of the PCC, the –OTf group (a good leaving group) departs, generating a tertiary carbocation at the bridgehead position (C_1). Subsequently, the $SiMe_3F$ (TMSF) moiety is eliminated, leading to the formation of the anti-Bredt olefin. This pathway closely resembles an E1-type elimination mechanism. A schematic representation of this mechanism is shown below:

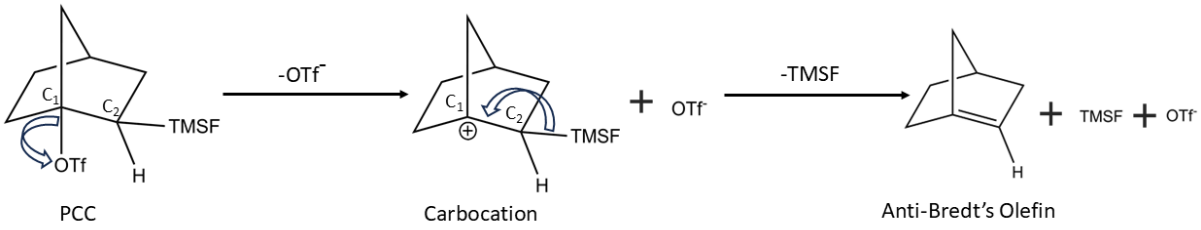

Figure S6: Mechanism-1 involves the initial removal of $–OTf^-$ leaving group, followed by the elimination of $SiMe_3F$ (TMSF), leading to the formation of the anti-Bredt olefin.

4.2 Mechanism-2:

Once the PCC is formed, elimination of the $SiMe_3F$ (TMSF) group (a stable species) produces a secondary carbanion adjacent to the bridgehead carbon (C_2). Subsequent loss of the –OTf group affords the anti-Bredt olefin through a pathway that closely follows an E1cb-type elimination mechanism. A schematic representation of this process is provided below.

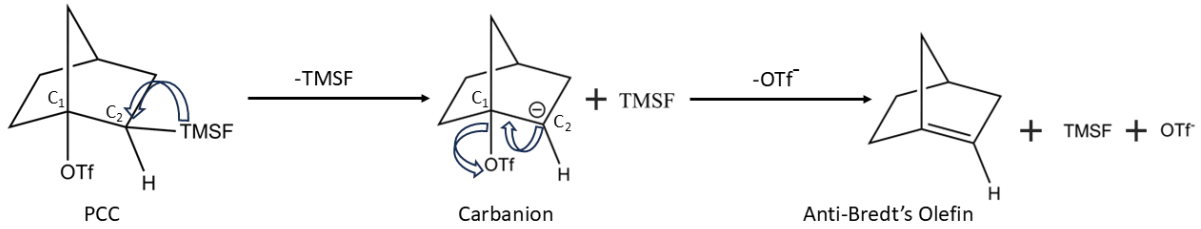

Figure S7: Mechanism-2 involves the initial removal of $SiMe_3F$ (TMSF), followed by the elimination of –OTf⁻ group, leading to the formation of the anti-Bredt olefin.

4.3 Mechanism-3:

In this mechanistic pathway, following the formation of the PCC, both the –OTf and $SiMe_3F$ (TMSF) groups are expelled nearly simultaneously (more like concerted mechanism). This elimination directly yields the anti-Bredt olefin. A schematic representation of this process is provided below.

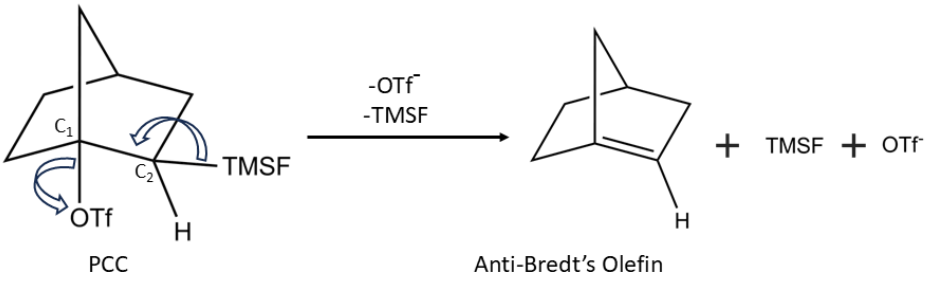

Figure S8: Mechanism-3, here both $SiMe_3F$ (TMSF) and -OTf⁻ group remove nearly simultaneously

These three possible mechanisms are clearly illustrated in the 2D potential energy surface (PES) scan for iso-1 (see Fig S4). The yellow line on the PES represents the minimum energy path (MEP), indicating that the formation of the anti-Bredt olefin proceeds via mechanism-3, in which both –OTf the and SiMe3F groups are removed nearly simultaneously. The PES further shows that the activation barrier for this process is ~12 kcal/mol.

The green and black dotted lines on the PES do not represent the minimum energy path (MEP); they are drawn manually to illustrate mechanism-1 and mechanism-2. From the PES, mechanism-1 (green dotted line) can be clearly observed, where the PCC generates a carbocation at the bridgehead (C_2) carbon upon release of –OTf. The formation of this carbocation is highly energy-demanding (activation energy barrier ~30 kcal/mol), as evident from the PES. Once the carbocation is formed, the anti-Bredt olefin can be produced relatively easily (activa-

tion energy barrier ~9 kcal/mol) through the release of the $SiMe_3F$ group, which is a low-energy process. Overall, mechanism-1 is not energetically favorable for the formation of the anti-Bredt olefin in iso-1 due to the high energy requirement for carbocation formation.

Mechanism-2 (black dotted line) is illustrated on the PES. In this pathway, the $SiMe_3F$ group is first released, leading to the formation of a carbanion at the C_2 carbon, with an associated activation energy of ~22 kcal/mol. Once the carbanion is formed, the anti-Bredt olefin can be generated readily through the loss of the –OTf leaving group, a process that is nearly barrierless.

Considering all possible mechanistic pathways, it is evident that the formation of the anti-Bredt olefin's from the PCC predominantly follows mechanism-3. This pathway is both energetically and kinetically favorable compared to the alternatives. Mechanism-1, involving carbocation formation at the bridgehead carbon, is highly energy-demanding (activation energy barrier ~30 kcal/mol), making it unfavorable despite the subsequent low-energy release of the $SiMe_3F$ group. Mechanism 2, which proceeds via carbanion formation at C_2, also requires a significant activation barrier of ~22 kcal/mol, even though the subsequent –OTf elimination is nearly barrierless. In contrast, mechanism-3 involves the concerted removal of both –OTf and $SiMe_3F$ groups, following the minimum energy path on the PES. The relatively low activation barrier (~12 kcal/mol) along this path ensures rapid and efficient formation of the anti-Bredt olefin, highlighting the preference of this pathway for iso-1.

5 Nudge Elastic Band Calculation

The Nudged Elastic Band (NEB) [11, 12] method is a computational technique used to determine the minimum energy path (MEP) between two known states on a potential energy surface (PES), typically a reactant and a product. The MEP provides valuable insight into the reaction coordinate and helps identify the location of the transition state (TS).

To construct the path, a series of intermediate structures, called images, are generated between the reactant and product geometries most often through linear interpolation of atomic coordinates. Together with the reactant and product states, these images form a discrete approximation of the reaction pathway.

The images are conceptually connected by virtual harmonic springs, creating an "elastic band." The role of these springs is to prevent the images from sliding into energy minima (reactant or product wells) and to maintain an approximately uniform spacing of images along the

path. Through iterative optimization, the NEB method refines the positions of the images to converge on the true MEP, locating the transition state and mapping the energy barrier.

We have done NEB for every step for the proposed energy diagram (Fig 2).

5.1 From iso-1 to B

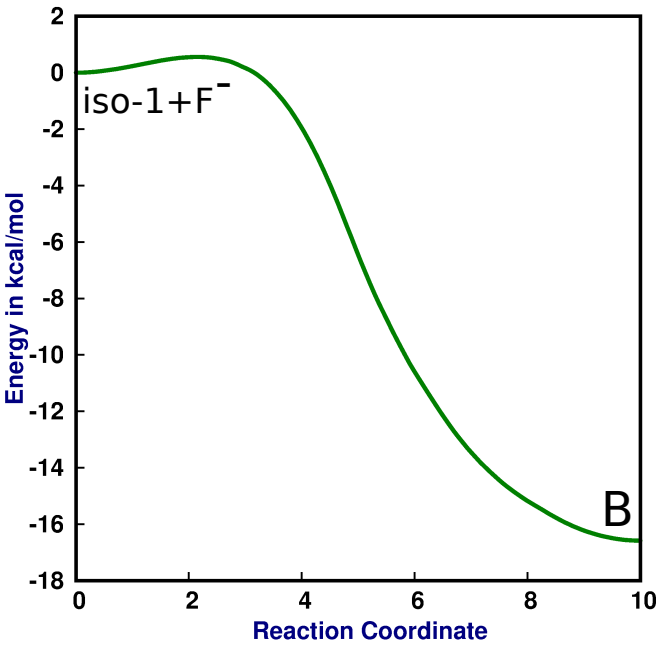

Figure S9: The minimum energy pathway (MEP) was elucidated through NEB calculations, starting from iso-1 with F^-. The results indicate that the reaction proceeds toward the formation of a stable PCC (B) with a very small thermal energy barrier of approximately 0.5 kcal mol^{-1}.

5.2 From B to C

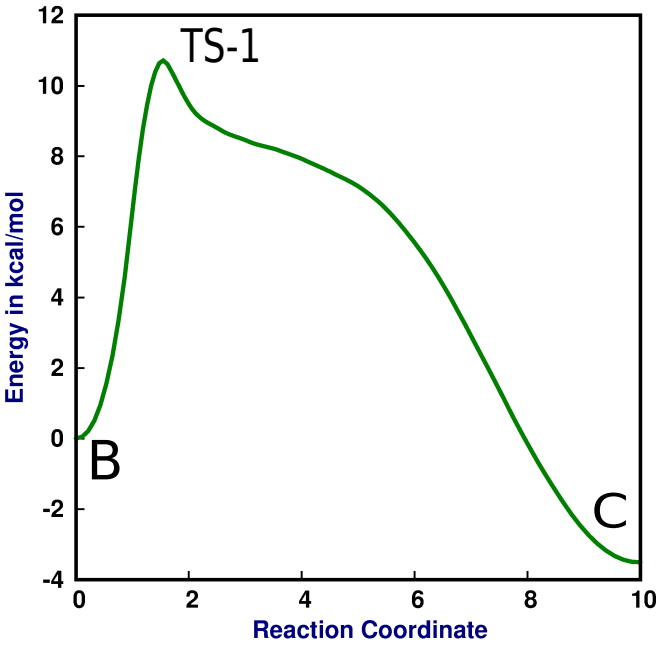

Figure S10: The minimum energy pathway (MEP) was elucidated through NEB calculations, starting from B. The results indicate that the reaction proceeds toward the formation of C via TS-1 with a thermal energy barrier of 10.61 kcal mol^{-1}

5.3 From iso-2 to D

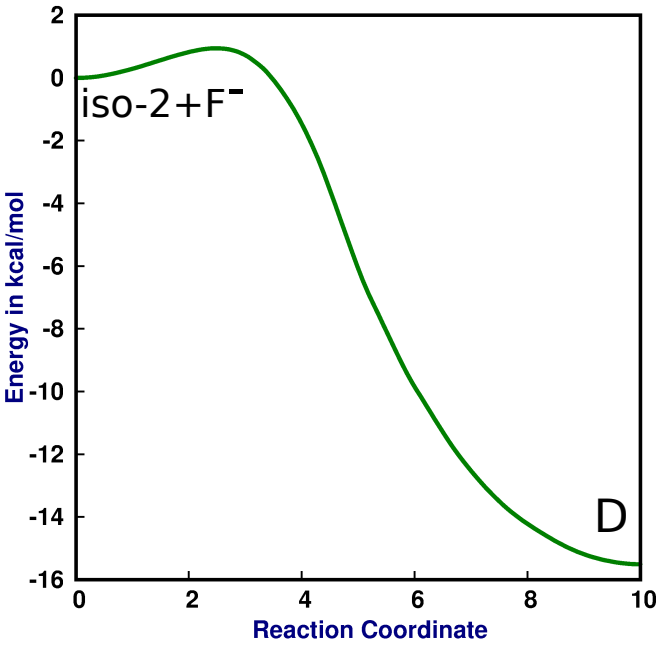

Figure S11: The minimum energy pathway (MEP) was elucidated through NEB calculations, starting from iso-2 with F^-. The results indicate that the reaction proceeds toward the formation of a stable PCC (D) with a very small thermal energy barrier of 0.94 kcal mol^{-1}..

5.4 From D to E

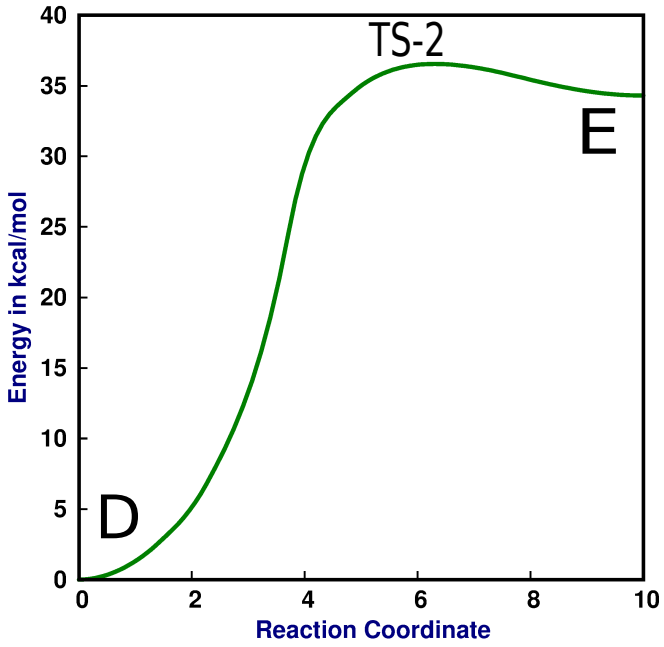

Figure S12: The minimum energy pathway (MEP) was elucidated through NEB calculations, starting from D. The results indicate that the reaction proceeds toward the formation of E via TS-2 with a very high thermal energy barrier of 36.55 kcal mol^{-1}.

5.5 From E to F

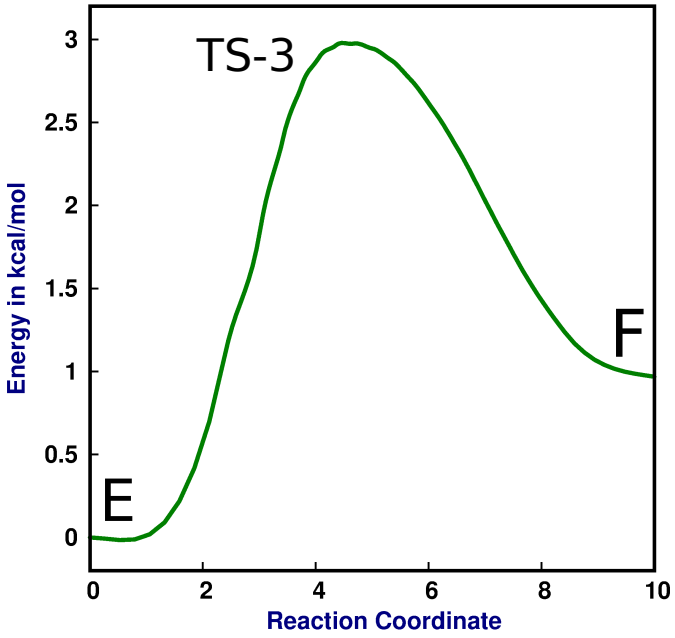

Figure S13: The minimum energy pathway (MEP) was elucidated through NEB calculations, starting from E. The results indicate that the reaction proceeds toward the formation of F via TS-3 with a low thermal energy barrier of 2.97 kcal mol^{-1}..

6 Rate Constant (k) calculation

All the rate constants (k) were calculated using the Eyring equation [13], given below-

$$k = \frac{\kappa k_B T}{hC^\circ} \exp\left(-\frac{\Delta G^\ddagger}{RT}\right) \tag{1}$$

Here,

$k =$ Rate constant (L/mol/s)

$\kappa =$ Transmission Coefficient (standard = 1)

$k_B =$ Boltzmann Constant (1.38×10^{-23} J/K)

$h =$ Planck's Constant (6.62×10^{-34} Js)

$C^\circ =$ Standard concentration (1 mol/L)

$\Delta G^\ddagger =$ Gibbs free energy of activation (J/mol)

$R =$ Gas constant (8.314 J/mol/K)

$T =$ Temperature (K)

7 Relation between Rate Constant (k) and Equilibrium Constant (K)

A general reaction in equilibrium can be represented as-

$$A \underset{k_2}{\overset{k_1}{\rightleftharpoons}} B$$

The equilibrium constant (K) is given by:

$$K = \frac{k_1}{k_2}$$

Here,

$k_1 =$ Forward reaction rate constant

$k_2 =$ Backward reaction rate constant

7.1 Equlibrium Constant (K) for B to C Process:

The equilibrium constant (K) is given by:

$$K = \frac{k_1}{k_2}$$

Here,

$k_1 =$ Forward reaction rate constant = 3.02*10^8

$k_2 =$ Backward reaction rate constant = 8.07*10^7

$$K = \frac{3.02 \times 10^8}{8.07 \times 10^7} = 3.74$$

7.2 Equlibrium Constant (K) for D to E Process:

The equilibrium constant (K) is given by:

$$K = \frac{k_1}{k_2}$$

Here,

k_1 = Forward reaction rate constant = 2.09*10^{-12}

k_2 = Backward reaction rate constant = 3.64*10^{10}

$$K = \frac{2.09 \times 10^{-12}}{3.64 \times 10^{10}} = 5.74 \times 10^{-23}$$

7.3 Equlibrium Constant (K) for E to F Process:

The equilibrium constant (K) is given by:

$$K = \frac{k_1}{k_2}$$

Here,

k_1 = Forward reaction rate constant = 1.11*10^{11}

k_2 = Backward reaction rate constant = 1.37*10^{11}

$$K = \frac{1.11 \times 10^{11}}{1.37 \times 10^{11}} = 0.81$$

8 Natural Bond Orbital (NBO) Partial Charge and Natural Atomic Orbital (NAO) Analysis

NBO analysis [14, 15] involves the transformation of the molecular wavefunction into natural atomic orbitals (NAOs), natural hybrid orbitals (NHOs), and natural bond orbitals (NBOs), which include bonding orbitals (σ and π bonds), lone pairs (nonbonding orbitals), antibonding orbitals, and Rydberg orbitals. NBOs represent an idealized Lewis-like bonding picture, where bonding orbitals have high occupancy (close to 2 electrons), lone pairs correspond to localized electron pairs on atoms, and antibonding orbitals have low occupancy, indicating deviations from perfect localization or delocalization effects. The analysis helps quantify covalency, hybridization, charge transfer, and hyperconjugation within molecules.

The partial charge for C_1 and C_2 for both iso-1 and iso-2 were calculated using NBO 7.0.10 program [16]. The tables are given below.

Table S3: The partial charge analysis of C_1 and C_2 in iso-1 was examined as a function of the Si–F distance (steps 1–25), followed by the C_1–OTf distance (steps 26–49)

iso-1: Partial Charge					
No. of steps	Si-F (Å)	C_1-OTf (Å)	C_2-Si (Å)	C_1	C_2
1	3.50	1.47	1.93	0.27623	-0.73129
2	3.42	1.47	1.93	0.27624	-0.73088
3	3.36	1.47	1.94	0.27625	-0.73048
4	3.28	1.47	1.94	0.27620	-0.72992
5	3.21	1.47	1.94	0.27613	-0.72957
6	3.14	1.47	1.94	0.27608	-0.72929
7	3.06	1.47	1.94	0.27603	-0.72914
8	2.99	1.47	1.95	0.27596	-0.72910
9	2.92	1.47	1.95	0.27587	-0.72935
10	2.85	1.47	1.96	0.27577	-0.72935
11	2.78	1.47	1.96	0.27559	-0.72939
12	2.70	1.47	1.97	0.27534	-0.72951
13	2.63	1.47	1.97	0.27513	-0.72963
14	2.56	1.48	1.98	0.27478	-0.72951
15	2.49	1.48	2.00	0.27438	-0.72918
16	2.41	1.48	2.00	0.27378	-0.72889
17	2.34	1.48	2.01	0.27302	-0.72825
18	2.27	1.48	2.02	0.27216	-0.72746
19	2.20	1.48	2.04	0.27116	-0.72629
20	2.12	1.49	2.05	0.27015	-0.72497
21	2.05	1.49	2.06	0.26917	-0.72284
22	1.98	1.49	2.08	0.26809	-0.72003
23	1.90	1.49	2.10	0.26700	-0.71704
24	1.83	1.49	2.11	0.26581	-0.71361
25	1.76	1.49	2.13	0.26449	-0.70980

iso-1: Partial Charge					
No. of steps	Si-F (Å)	C_1-OTf (Å)	C_2-Si (Å)	C_1	C_2
26	1.77	1.49	2.13	0.26482	-0.71076
27	1.77	1.53	2.13	0.26367	-0.71066
28	1.77	1.57	2.14	0.26271	-0.70983
29	1.77	1.61	2.15	0.26145	-0.70770
30	1.77	1.64	2.16	0.25957	-0.70390
31	1.76	1.68	2.18	0.25727	-0.69803
32	1.76	1.71	2.19	0.25483	-0.69282
33	1.76	1.76	2.21	0.25042	-0.68289
34	1.75	1.79	2.23	0.24672	-0.67482
35	1.75	1.83	2.27	0.23981	-0.65932
36	1.74	1.87	2.33	0.22886	-0.63648
37	1.73	1.90	2.38	0.21896	-0.61656
38	1.72	1.94	2.45	0.20628	-0.59186
39	1.71	1.98	2.55	0.18959	-0.56092
40	1.70	2.01	2.68	0.16968	-0.52569
41	1.70	2.05	2.77	0.15516	-0.49964
42	1.70	2.09	2.84	0.14420	-0.47897
43	1.69	2.13	2.89	0.13533	-0.46148
44	1.69	2.17	2.94	0.12773	-0.44597
45	1.69	2.20	2.97	0.12207	-0.43330
46	1.69	2.24	2.99	0.11635	-0.42175
47	1.68	2.28	3.06	0.10999	-0.40746
48	1.68	2.31	3.07	0.10688	-0.39892
49	1.68	2.35	3.09	0.10363	-0.39059

Table S4:The partial charge analysis of C_1 and C_2 in iso-2 was examined as a function of the Si–F distance (steps 1–25), followed by the C_1–OTf distance (steps 26–55) and by C_2–Si distance (steps 56-66)

iso-2: Partial Charge					
No. of steps	Si-F (Å)	C_1-OTf (Å)	C_2-Si (Å)	C_1	C_2
1	3.50	1.47	1.92	0.28122	-0.73694
2	3.43	1.47	1.93	0.28123	-0.73650
3	3.36	1.47	1.93	0.28130	-0.73617
4	3.28	1.47	1.93	0.28127	-0.73577
5	3.21	1.47	1.94	0.28124	-0.73552
6	3.14	1.47	1.94	0.28114	-0.73532
7	3.07	1.47	1.94	0.28105	-0.73534
8	2.99	1.47	1.94	0.28097	-0.73545
9	2.92	1.47	1.95	0.28086	-0.73561
10	2.85	1.47	1.95	0.28073	-0.73592
11	2.78	1.47	1.96	0.28058	-0.73645
12	2.70	1.47	1.96	0.28048	-0.73710
13	2.63	1.47	1.97	0.28022	-0.73762
14	2.56	1.47	1.98	0.27981	-0.73786
15	2.49	1.47	1.99	0.27947	-0.73801
16	2.41	1.48	2.00	0.27911	-0.73795
17	2.34	1.48	2.01	0.27848	-0.73707
18	2.27	1.48	2.02	0.27805	-0.73604
19	2.20	1.48	2.03	0.27766	-0.73512
20	2.12	1.48	2.04	0.27726	-0.73389
21	2.05	1.48	2.05	0.27691	-0.73220
22	1.98	1.48	2.06	0.27641	-0.73037
23	1.91	1.48	2.08	0.27596	-0.72823
24	1.83	1.48	2.09	0.27543	-0.72568
25	1.76	1.48	2.11	0.27493	-0.72326
26	1.78	1.49	2.11	0.27477	-0.72421
27	1.78	1.55	2.11	0.27646	-0.72909
28	1.78	1.62	2.11	0.27957	-0.73313

iso-2: Partial Charge					
No. of steps	Si-F (Å)	C_1-OTf (Å)	C_2-Si (Å)	C_1	C_2
29	1.78	1.68	2.11	0.28355	-0.73636
30	1.78	1.75	2.11	0.28815	-0.73873
31	1.78	1.82	2.12	0.29317	-0.74011
32	1.78	1.88	2.12	0.29854	-0.74041
33	1.77	1.95	2.12	0.30393	-0.73962
34	1.77	2.02	2.12	0.30891	-0.73715
35	1.77	2.08	2.13	0.31317	-0.73232
36	1.77	2.15	2.13	0.31678	-0.72685
37	1.76	2.21	2.14	0.31910	-0.71929
38	1.76	2.28	2.14	0.32097	-0.71165
39	1.76	2.35	2.15	0.32297	-0.70465
40	1.76	2.41	2.16	0.32516	-0.69853
41	1.75	2.48	2.19	0.32763	-0.69047
42	1.75	2.54	2.19	0.33024	-0.68638
43	1.75	2.61	2.20	0.33186	-0.68146
44	1.75	2.68	2.20	0.33421	-0.67861
45	1.74	2.74	2.20	0.33594	-0.67573
46	1.74	2.81	2.20	0.33726	-0.67328
47	1.74	2.88	2.20	0.33915	-0.67223
48	1.74	2.94	2.20	0.33902	-0.67005
49	1.74	3.01	2.20	0.33951	-0.66906
50	1.74	3.07	2.20	0.34051	-0.66859
51	1.74	3.14	2.20	0.33952	-0.66721
52	1.74	3.21	2.20	0.33905	-0.66651
53	1.74	3.27	2.20	0.33865	-0.66587
54	1.74	3.34	2.21	0.33276	-0.66288
55	1.74	3.47	2.21	0.33207	-0.67774
56	1.73	3.59	2.31	0.31809	-0.64182
57	1.72	3.59	2.47	0.29968	-0.60803
58	1.70	3.60	2.63	0.27465	-0.56935

No. of steps	Si-F (Å)	C_1-OTf (Å)	C_2-Si (Å)	C_1	C_2
59	1.69	3.60	2.79	0.24519	-0.52865
60	1.69	3.60	2.94	0.21660	-0.49105
61	1.68	3.59	3.11	0.18582	-0.45903
62	1.68	3.61	3.26	0.16371	-0.43780
63	1.67	3.61	3.42	0.15197	-0.42632
64	1.67	3.63	3.58	0.14850	-0.42142
65	1.67	3.64	3.74	0.14419	-0.41400
66	1.67	3.61	3.89	0.13759	-0.40301

Natural Atomic Orbital (NAO) [17, 18] energies are obtained within the framework of the chosen quantum chemical method such as Hartree–Fock or Kohn–Sham density functional theory. The calculation begins by solving the self-consistent field (SCF) equations, which provide the molecular Fock (or Kohn–Sham) matrix in the chosen basis set.

NBO analysis then constructs an atom-centered, orthonormal basis of NAOs by projecting and orthogonalizing the original atomic basis functions. This ensures that the resulting orbitals are localized on atoms and resemble the natural one-electron environment of each atom.

Once the NAO basis is defined, the Fock matrix is transformed into this representation. The diagonal elements of this transformed matrix correspond to the NAO orbital energies, expressed in atomic units (hartree).

Table S5: The Natural Atomic Orbital (NAO) analysis of the valence-shell atomic orbitals of C_1 and C_2 in iso-1, as a function of the C_1–OTf distance, provides a description of the orbital energies expressed in Hartree units.

C_1-OTf (Å)	C_1				C_2			
	2s	2p$_x$	2p$_y$	2p$_z$	2s	2p$_x$	2p$_y$	2p$_z$
1.42	0.00619	0.04047	0.06165	0.03425	-0.0075	0.05137	0.08319	0.08469
1.45	-0.0016	0.03937	0.05249	0.03371	-0.0074	0.05045	0.08212	0.08372
1.49	-0.0080	0.03860	0.04425	0.03348	-0.0072	0.04949	0.08100	0.08271
1.53	-0.0133	0.03813	0.03690	0.03356	-0.0070	0.04857	0.07989	0.08174
1.56	-0.0175	0.03791	0.03031	0.03385	-0.0069	0.04749	0.07863	0.08063
1.60	-0.0207	0.03806	0.02466	0.03453	-0.0067	0.04657	0.07750	0.07967
1.64	-0.0225	0.03871	0.02001	0.03573	-0.0061	0.04587	0.07657	0.07895
1.68	-0.0234	0.03957	0.01618	0.03724	-0.0054	0.04540	0.07558	0.07824
1.71	-0.0238	0.04039	0.01276	0.03863	-0.0052	0.04413	0.07415	0.07706
1.75	-0.0227	0.04214	0.01077	0.04100	-0.0037	0.04382	0.07370	0.07689
1.79	-0.0218	0.04340	0.00870	0.04284	-0.0035	0.04252	0.07227	0.07578

Table S6: The Natural Atomic Orbital (NAO) analysis of the valence-shell atomic orbitals of C_1 and C_2 in iso-2, as a function of the C_1–OTf distance, provides a description of the orbital energies expressed in Hartree units.

C_1-OTf (Å)	C_1				C_2			
	2s	2p$_x$	2p$_y$	2p$_z$	2s	2p$_x$	2p$_y$	2p$_z$
1.42	0.0034	0.05314	0.04464	0.03446	-0.0123	0.08318	0.06124	0.06932
1.48	-0.0111	0.04424	0.03716	0.03060	-0.0126	0.08134	0.05952	0.06726
1.55	-0.0222	0.03684	0.03108	0.02758	-0.0134	0.07938	0.05761	0.06506
1.61	-0.0308	0.03066	0.02613	0.02521	-0.0147	0.07723	0.05545	0.06272
1.68	-0.0372	0.02562	0.02221	0.02344	-0.0162	0.07497	0.05311	0.06035
1.75	-0.0417	0.02157	0.01910	0.02211	-0.0179	0.07260	0.05057	0.05797
1.79	-0.0439	0.01946	0.01746	0.02124	-0.0191	0.07107	0.04896	0.05649
1.81	-0.0449	0.01838	0.01660	0.02137	-0.0198	0.07010	0.04739	0.05563
1.88	-0.0470	0.01589	0.01456	0.02089	-0.0219	0.06767	0.04511	0.05333

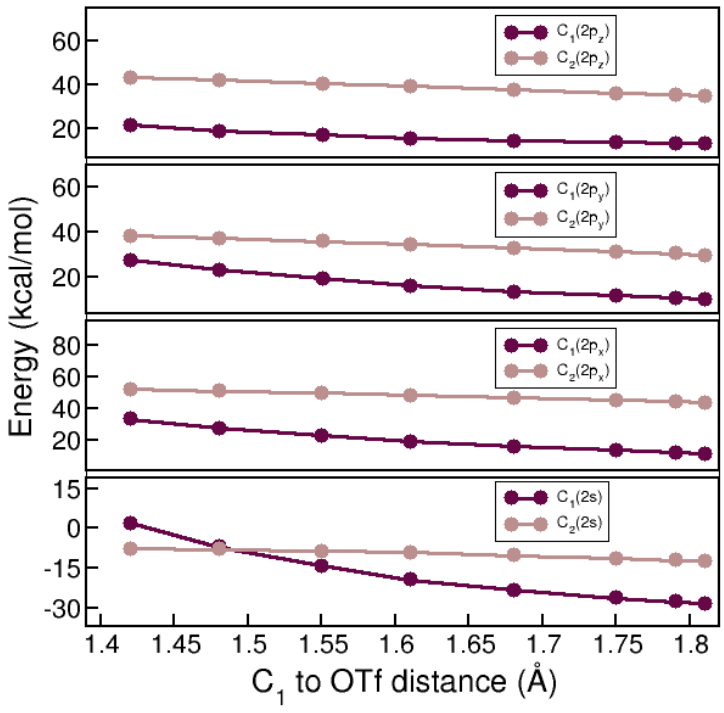

Figure S14: Energy levels of the atomic orbitals for C_1 (maroon) and C_2 (brown) in iso-2 respect to C_1-OTf distance. Here, it is clear that none of the same-symmetry atomic orbitals in this system match closely in energy, and therefore they remain essentially non-interacting.

9 Structural features Of Pentacoordinated Siliconate complex (PCC) of iso-1

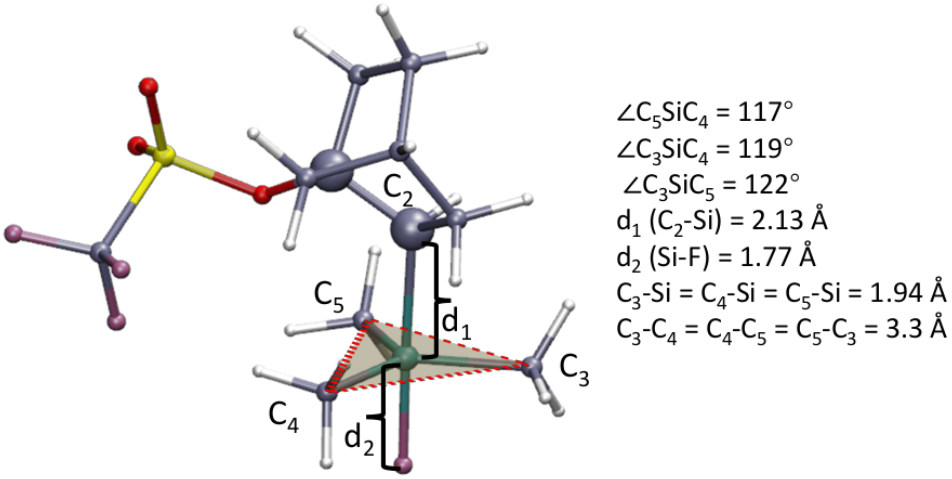

Figure S15: Coordination of F^- to the silicon center of the TMS group results in the formation of a stable pentacoordinated siliconate complex (PCC). The optimized structure reveals that the PCC adopts a trigonal bipyramidal (TBP) geometry, with the fluoride ion occupying an axial position. All structural features of TBP are illustrated in this image.

10 Partial charge analysis of Pentacoordinated complexes by NBO

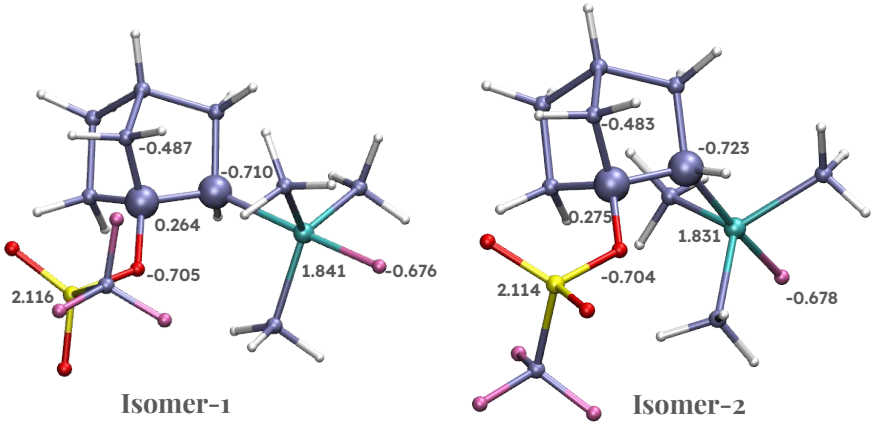

Figure S16: The NBO partial charge analysis was performed for the PCC structures formed from iso-1 and iso-2. The results indicate that silicon acts as a highly electropositive center in both complexes.

11 Coordinates of all the optimised structures

All the structures were optimised and the Hessian calculation was done, the coordinates of the optimized structure are given below . In some structure there were imaginary modes corresponding to methyl group rotation which were being neglected.

- Coordinates of iso-1

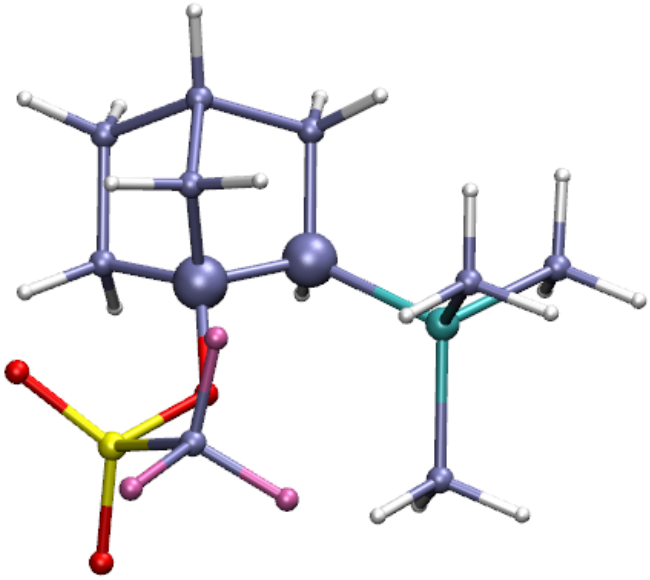

SPE:-1642.6579 Eh, Gibbs Free Energy: -1642.4485 Eh

Atomic coordinates of iso-1

Atom	X	Y	Z
C	-0.703663	0.469744	-0.376431
C	0.813992	0.354986	-0.124737
C	0.521232	2.569165	-0.075408
C	-0.898535	2.018664	-0.384270
H	-0.989940	-0.022563	-1.326226
H	-1.267486	-0.006997	0.447237
H	-1.283759	2.398634	-1.351738
H	-1.617068	2.329256	0.399898
C	1.081202	1.494486	0.879108
H	2.155193	1.622601	1.109109
H	0.508092	1.378088	1.818058
C	1.572487	0.804726	-1.400939
H	1.029340	0.411919	-2.287841
C	1.420551	2.364283	-1.316720
H	2.398784	2.868584	-1.163403

Continued on next page

Atom	X	Y	Z
H	0.977904	2.794729	-2.237050
H	0.522244	3.606078	0.312284
Si	3.379914	0.208098	-1.635382
C	3.995722	1.086327	-3.200504
H	3.374239	0.818831	-4.080466
H	3.972697	2.190330	-3.092610
C	4.483416	0.711744	-0.180126
H	4.197276	0.194095	0.755204
H	4.452192	1.805154	0.005899
C	3.454264	-1.661566	-1.905782
H	2.759181	-1.970861	-2.713653
H	3.168486	-2.210027	-0.988454
O	1.270431	-0.992141	0.212154
S	0.820376	-1.779925	1.577475
O	-0.177437	-1.031030	2.358933
O	0.664874	-3.189996	1.217186
C	2.456871	-1.662067	2.531032
F	2.749235	-0.379057	2.795283
F	3.447930	-2.203533	1.814221
F	2.318498	-2.328222	3.680824
H	5.537926	0.444022	-0.400990
H	5.042162	0.793480	-3.426915
H	4.477593	-1.974166	-2.200773

- Coordinates of (B)

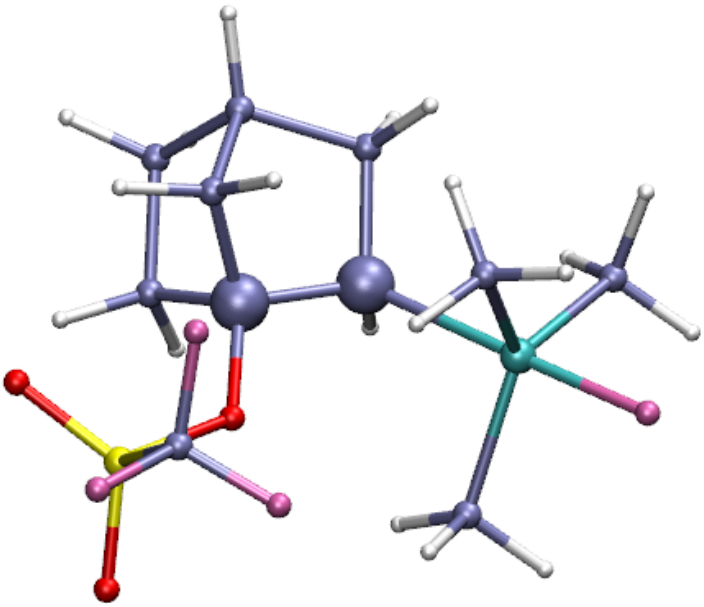

SPE:-1742.4856 Eh, Gibbs Free Energy:-1742.2680 Eh

Atomic coordinates of (B)

Atom	X	Y	Z
C	-0.308284	0.751421	0.129486
C	1.214090	0.507873	0.200278
C	1.138237	2.726314	0.317028
C	-0.351717	2.313856	0.130988
H	-0.738979	0.297376	-0.784493
H	-0.830075	0.333108	1.014883
H	-0.771919	2.730427	-0.807999
H	-0.975024	2.691317	0.968574
C	1.670629	1.584086	1.205242
H	2.767185	1.599407	1.332138
H	1.171358	1.498692	2.190276
C	1.882599	0.888621	-1.128350
H	1.187220	0.596607	-1.946812
C	1.902741	2.446617	-0.996795
H	2.944263	2.837664	-0.921888

Continued on next page

Atom	X	Y	Z
H	1.435126	2.959870	-1.863742
H	1.263091	3.752269	0.724089
Si	3.708505	0.040788	-1.823759
C	3.614830	1.214926	-3.363196
H	2.598659	1.568261	-3.637471
H	4.240147	2.116473	-3.178620
C	4.676789	0.623822	-0.249827
H	4.466859	-0.071553	0.589593
H	4.410188	1.644539	0.097210
C	2.907950	-1.710141	-1.970497
H	1.799496	-1.725138	-1.997232
H	3.213860	-2.315412	-1.090545
O	1.547936	-0.909546	0.537102
S	1.172752	-1.628812	1.925934
O	0.357913	-0.800304	2.839026
O	0.813813	-3.024391	1.638713
C	2.893290	-1.714363	2.713707
F	3.348771	-0.485500	2.998748
F	3.758431	-2.335067	1.907115
F	2.793121	-2.410459	3.864678
H	5.767089	0.592043	-0.444090
H	4.066127	0.691719	-4.230716
H	3.310943	-2.219852	-2.869944
F	5.222731	-0.638982	-2.449750

- Coordinates of TS-1:

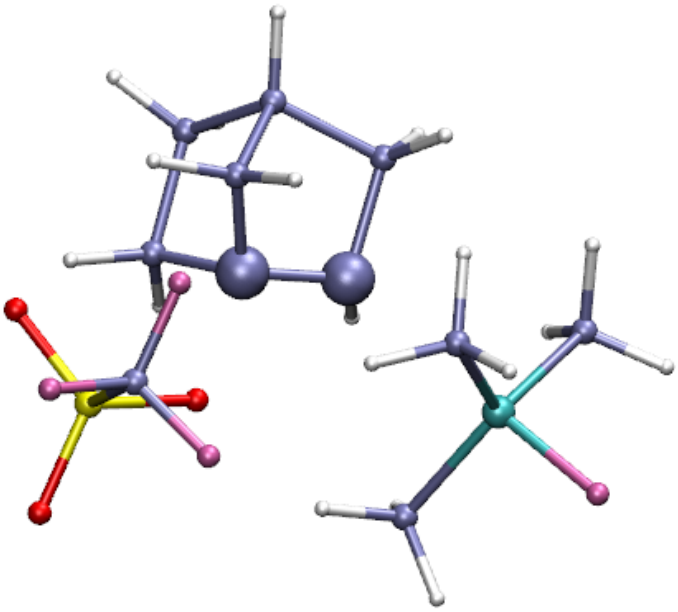

SPE: -1742.4943 Eh, Gibbs Free Energy: -1742.2586 Eh,

Atomic coordinates of TS-1

Atom	X	Y	Z
C	-2.496400	0.232009	0.364892
C	-0.990047	0.196634	0.289119
C	-1.114510	2.334986	0.558643
C	-2.594489	1.821534	0.366575
H	-2.981152	-0.217596	-0.523396
H	-2.903583	-0.214511	1.293413
H	-3.040592	2.205182	-0.575193
H	-3.226921	2.173092	1.208651
C	-0.529014	1.169392	1.376211
H	0.569195	1.205684	1.490751
H	-1.008874	0.973102	2.353168
C	-0.429718	0.594619	-0.947299
H	-1.031550	0.310586	-1.830723
C	-0.281338	2.127146	-0.746233
H	0.761920	2.505129	-0.600880

Continued on next page

Atom	X	Y	Z
H	-0.694562	2.668924	-1.624092
H	-1.065128	3.353212	1.007897
Si	1.785713	-0.558973	-1.925919
C	1.568081	0.876926	-3.162801
H	0.564283	0.863853	-3.633368
H	1.694616	1.864295	-2.674568
C	2.446750	-0.147703	-0.200991
H	1.897313	-0.743041	0.553239
H	2.319287	0.924620	0.049148
C	0.594710	-2.022802	-2.100386
H	-0.274295	-1.773023	-2.742820
H	0.209088	-2.316645	-1.104240
O	-0.413383	-1.619531	0.961268
S	-0.844122	-2.184457	2.322743
O	-1.819742	-1.338036	3.066039
O	-1.078509	-3.646867	2.294435
C	0.751089	-2.002887	3.328370
F	1.093213	-0.704820	3.486314
F	1.779681	-2.632789	2.725525
F	0.595048	-2.540284	4.558753
H	3.527627	-0.394769	-0.143525
H	2.334001	0.784782	-3.961300
H	1.135587	-2.877302	-2.558917
F	3.190727	-1.249672	-2.598502

- Coordinates of (C):

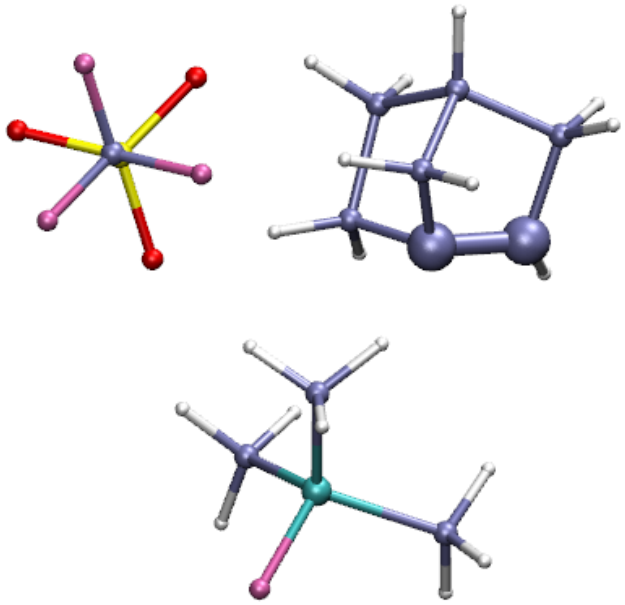

SPE:-1742.4962 Eh, Gibbs Free Energy:-1742.2692 Eh,

Atomic coordinates of (C)

Atom	X	Y	Z
C	0.451988	0.698786	-0.678965
C	1.596937	1.682543	-0.832864
C	0.657033	2.802892	0.761998
C	-0.330689	1.625159	0.375509
H	-0.139124	0.550745	-1.604984
H	0.740449	-0.270467	-0.229875
H	-1.288568	1.997871	-0.046737
H	-0.520859	1.026647	1.287918
C	1.986643	2.045151	0.609323
H	2.885558	2.690978	0.682131
H	2.071365	1.169399	1.279581
C	1.291026	2.843636	-1.499831
H	0.730515	2.815960	-2.452085
C	0.873895	3.842214	-0.406705
H	1.602780	4.629237	-0.095023

Continued on next page

Atom	X	Y	Z
H	-0.046147	4.373417	-0.737979
H	0.416938	3.247053	1.753718
Si	4.129863	-0.871518	-2.181719
C	4.301519	0.495112	-3.474789
H	4.081609	0.127162	-4.498836
H	3.586174	1.310080	-3.233661
C	4.545534	-0.247093	-0.466978
H	4.030458	-0.864104	0.296682
H	4.185222	0.792834	-0.339518
C	2.465959	-1.726433	-2.311134
H	1.663238	-0.976732	-2.458124
H	2.238133	-2.267850	-1.370133
O	2.026716	-1.787791	0.917208
S	1.460256	-1.652489	2.304085
O	0.806956	-0.333345	2.591770
O	0.762952	-2.853923	2.834267
C	3.025425	-1.551575	3.368782
F	3.794670	-0.488465	3.020177
F	3.789253	-2.661353	3.240665
F	2.720275	-1.416004	4.680528
H	5.641286	-0.261197	-0.292797
H	5.324600	0.926223	-3.473177
H	2.450668	-2.429379	-3.170003
F	5.280235	-2.014804	-2.579344

- Coordinates of iso-2:

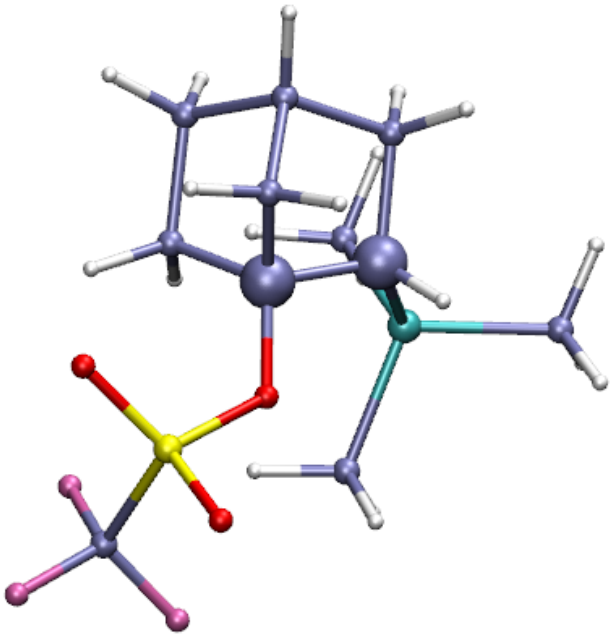

SPE:-1642.6684 Eh, Gibbs Free Energy:-1642.4451 Eh,

Atomic coordinates of iso-2

Atom	X	Y	Z
C	-0.145908	0.504687	0.375934
C	1.350484	0.736249	0.090878
C	0.527580	2.800617	-0.155093
C	-0.726338	1.936826	0.158933
H	-0.585345	-0.260423	-0.290294
H	-0.284859	0.165936	1.418562
H	-1.466244	1.976477	-0.665440
H	-1.232312	2.298948	1.075668
C	1.600763	2.123867	0.721362
H	2.630722	2.488992	0.536539
H	1.381516	2.149732	1.805650
C	1.596261	1.001750	-1.417475
H	2.701250	1.031405	-1.537267
C	1.018921	2.451784	-1.582253
H	1.805959	3.157023	-1.916587

Continued on next page

Atom	X	Y	Z
H	0.191675	2.515045	-2.318458
H	0.373605	3.883602	0.013343
Si	0.996706	-0.282416	-2.705087
C	1.994737	0.059844	-4.279278
H	3.080845	-0.089488	-4.106919
H	1.847048	1.103781	-4.626427
C	-0.844335	-0.080513	-3.127218
H	-1.510510	-0.257013	-2.258839
H	-1.066400	0.931080	-3.524957
C	1.323114	-2.044284	-2.101245
H	2.374965	-2.165521	-1.774060
H	0.675812	-2.307302	-1.241688
O	2.257182	-0.342172	0.471532
S	2.441362	-0.833096	2.026393
O	1.600652	-0.065201	2.960083
O	3.872136	-1.054062	2.242454
C	1.660777	-2.556326	1.860834
F	2.363380	-3.294095	0.998708
F	0.392299	-2.453357	1.432107
F	1.672606	-3.135658	3.065339
H	-1.123126	-0.812324	-3.914224
H	1.124841	-2.776176	-2.911856
H	1.686369	-0.615869	-5.103909

- Coordinates of (D):

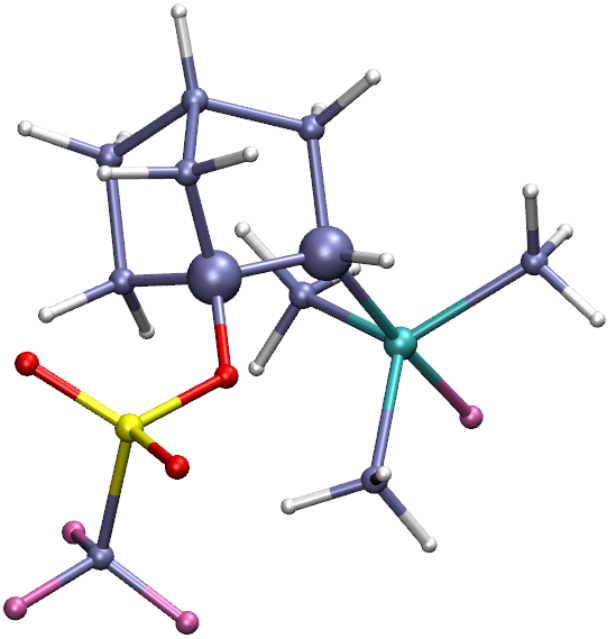

SPE:-1742.3045 Eh, Gibbs Free Energy:-1742.2644Eh,

Atomic coordinates of (D)

Atom	X	Y	Z
C	-0.641695	0.389251	0.106281
C	0.827152	0.819178	-0.083079
C	-0.241050	2.682055	-0.663410
C	-1.388401	1.695261	-0.311303
H	-0.885814	-0.477959	-0.531425
H	-0.848410	0.133072	1.161887
H	-2.070212	1.537357	-1.171129
H	-1.995178	2.089145	0.531207
C	0.814349	2.292322	0.387989
H	1.799618	2.779055	0.239033
H	0.478723	2.425261	1.437679
C	1.200255	0.896422	-1.581947
H	2.294150	1.111712	-1.589467
C	0.441048	2.211227	-1.975841
H	1.134433	2.995215	-2.349001

Continued on next page

Atom	X	Y	Z
H	-0.310981	2.044004	-2.778173
H	-0.561811	3.744614	-0.663046
Si	1.022329	-0.656891	-2.992440
C	2.039868	0.413104	-4.252097
H	3.004172	-0.108032	-4.440554
H	2.267833	1.459626	-3.959514
C	-0.914083	-0.612623	-3.107726
H	-1.297374	-1.582253	-2.720077
H	-1.456941	0.202262	-2.588862
C	1.902823	-1.911671	-1.815094
H	2.724853	-1.462682	-1.222508
H	1.162849	-2.301072	-1.081895
O	1.838257	-0.022587	0.599611
S	1.840106	-0.329923	2.181515
O	0.788698	0.379180	2.937695
O	3.236920	-0.333388	2.637176
C	1.331122	-2.157329	2.153720
F	2.261694	-2.893442	1.543067
F	0.151780	-2.324146	1.539771
F	1.212959	-2.573001	3.431527
H	-1.193838	-0.588899	-4.181429
H	2.285256	-2.777600	-2.391593
H	1.506513	0.422094	-5.225957
F	0.952107	-1.924524	-4.244748

- Coordinates of TS-2:

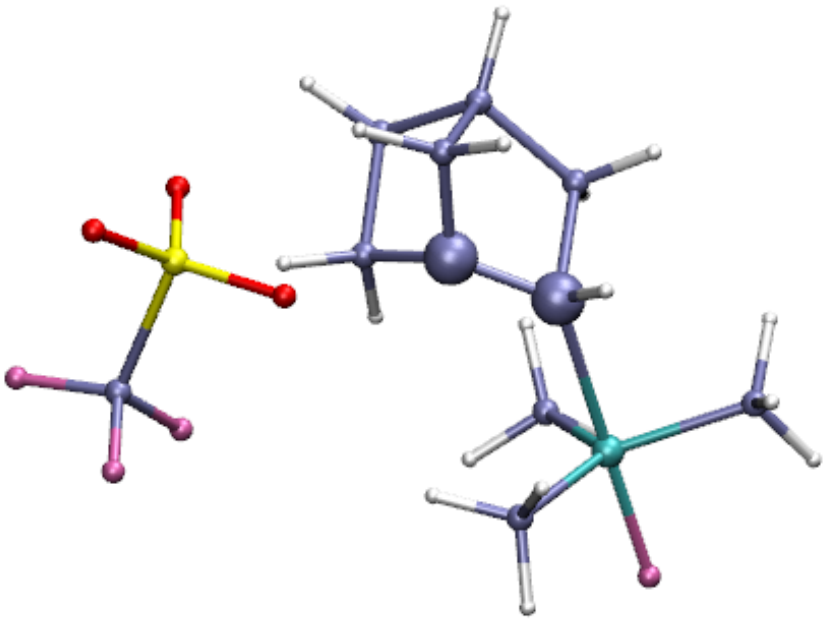

SPE:-1742.4464 Eh, Gibbs Free Energy:-1742.2112 Eh,

Atomic coordinates of TS-2

Atom	X	Y	Z
C	-0.919294	-0.089216	0.791920
C	0.356620	0.486006	0.244862
C	-0.607600	2.258223	0.540220
C	-1.633800	1.264326	1.141332
H	-1.450348	-0.713812	0.055369
H	-0.674052	-0.677588	1.695495
H	-2.634663	1.343806	0.669597
H	-1.719017	1.382369	2.238429
C	0.732321	1.665359	1.109463
H	1.642211	2.190552	0.765557
H	0.695043	1.489649	2.200948
C	0.609262	0.637238	-1.152728
H	1.601451	1.119866	-1.291098
C	-0.452445	1.874716	-1.008010
H	0.047513	2.691529	-1.561268

Continued on next page

Atom	X	Y	Z
H	-1.429115	1.639591	-1.475591
H	-0.797006	3.334475	0.730390
Si	0.371930	-0.798515	-2.836471
C	0.881439	0.678207	-3.956981
H	1.927445	0.990553	-3.747755
H	0.237222	1.568547	-3.796080
C	-1.505396	-1.042293	-2.518098
H	-1.648123	-1.963269	-1.912218
H	-2.040139	-0.217726	-2.005339
C	1.670586	-1.815172	-1.847147
H	2.558160	-1.208615	-1.570490
H	1.220066	-2.164397	-0.893405
O	1.399262	-1.043354	2.733675
S	0.873119	-0.571473	4.057480
O	-0.046126	0.620281	3.973586
O	1.842397	-0.555370	5.183356
C	-0.331056	-1.954229	4.541923
F	0.304486	-3.137659	4.687689
F	-1.294681	-2.125218	3.596802
F	-0.958723	-1.679101	5.708179
H	-2.000054	-1.227349	-3.493254
H	2.006778	-2.695966	-2.430019
H	0.818635	0.384685	-5.023850
F	0.345693	-1.939658	-4.146472

- Coordinates of (E):

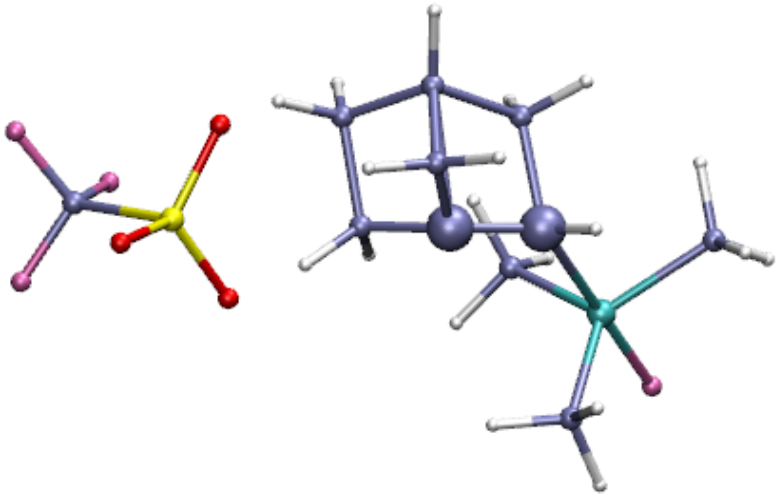

SPE:-1742.4480 Eh, Gibbs Free Energy:-1742.2160 Eh

Atomic coordinates of (E)

Atom	X	Y	Z
C	0.248191	-0.314376	-0.222795
C	1.304128	0.516940	-0.874188
C	0.150811	2.077550	-0.267333
C	-0.631162	0.876605	0.323477
H	-0.267832	-0.990399	-0.923596
H	0.708608	-0.867002	0.631593
H	-1.673779	0.820441	-0.050047
H	-0.615688	0.899851	1.428871
C	1.629094	1.650439	0.071124
H	2.397552	2.347610	-0.311565
H	1.746069	1.394669	1.141615
C	1.335850	0.843528	-2.266559
H	2.229049	1.475366	-2.466613
C	0.155713	1.898445	-1.855817
H	0.475456	2.834551	-2.350878

Continued on next page

Atom	X	Y	Z
H	-0.835093	1.584980	-2.240606
H	-0.162536	3.081325	0.083848
Si	1.031179	-0.442495	-4.044825
C	1.208773	1.182282	-5.056541
H	2.224221	1.618108	-4.936494
H	0.482264	1.956340	-4.729897
C	-0.739403	-0.960719	-3.513464
H	-0.697097	-1.990248	-3.096384
H	-1.257439	-0.319962	-2.772750
C	2.566062	-1.383142	-3.361161
H	3.404088	-0.700076	-3.108933
H	2.280659	-1.901613	-2.420139
O	1.839608	-1.066687	2.311880
S	1.403279	-0.256380	3.500187
O	0.888112	1.116393	3.163815
O	2.280783	-0.341744	4.695581
C	-0.173726	-1.155426	4.045177
F	0.083517	-2.433833	4.400324
F	-1.089897	-1.190627	3.040814
F	-0.756935	-0.545327	5.102154
H	-1.369375	-1.021860	-4.424505
H	2.924545	-2.138818	-4.088509
H	1.047073	0.979365	-6.133940
F	0.939356	-1.450661	-5.457077

- Coordinates of TS-3:

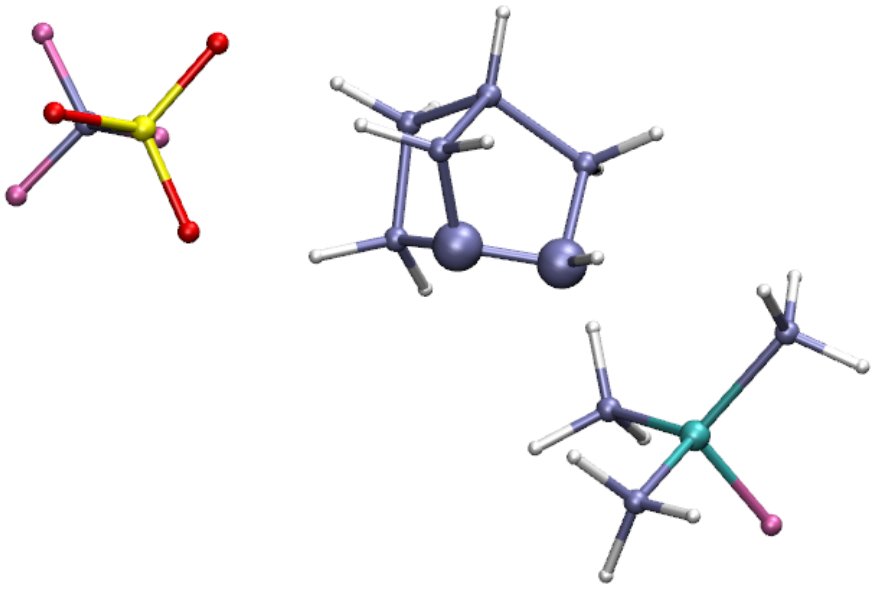

SPE:-1742.4439 Eh, Gibbs Free Energy:-1742.2122 Eh,

Atomic coordinates of TS-3

Atom	X	Y	Z
C	-0.330067	-0.400350	0.808899
C	0.760298	0.461298	0.230670
C	-0.585121	1.983280	0.788580
C	-1.273317	0.729824	1.371294
H	-0.801945	-1.046156	0.044696
H	0.080494	-1.007802	1.645093
H	-2.322823	0.617073	1.026290
H	-1.230552	0.737770	2.476792
C	0.945540	1.638905	1.165591
H	1.663879	2.401327	0.807501
H	1.040533	1.419209	2.247343
C	0.664671	0.939133	-1.090508
H	1.497989	1.637890	-1.320578
C	-0.618565	1.797319	-0.811458
H	-0.478548	2.753435	-1.356461

Continued on next page

Atom	X	Y	Z
H	-1.606298	1.387374	-1.121281
H	-0.977371	2.947617	1.179039
Si	0.315219	-0.936208	-3.534864
C	0.655021	0.778227	-4.260404
H	1.419947	1.332628	-3.685668
H	-0.270490	1.390071	-4.265563
C	-1.407529	-1.169766	-2.804501
H	-1.521464	-2.200873	-2.410186
H	-1.616568	-0.461362	-1.983152
C	1.720879	-1.772358	-2.590994
H	2.676595	-1.226857	-2.729320
H	1.518086	-1.815046	-1.505398
O	1.283982	-1.138539	3.406369
S	0.715598	-0.424568	4.596920
O	0.105318	0.917711	4.302147
O	1.525078	-0.500427	5.842585
C	-0.809420	-1.475207	5.009373
F	-0.467740	-2.748139	5.317841
F	-1.670889	-1.533347	3.958605
F	-1.494990	-0.971846	6.062826
H	-2.169029	-1.026192	-3.599693
H	1.851426	-2.803885	-2.981746
H	0.999683	0.667667	-5.310689
F	0.212487	-1.878829	-4.925995

- Coordinates of (F):

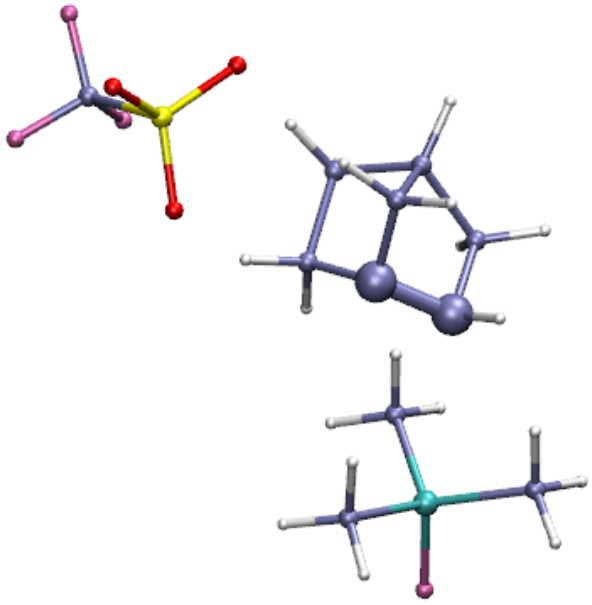

SPE:-1742.4471 Eh, Gibbs Free Energy:-1742.2158 Eh

Atomic coordinates of (F)

Atom	X	Y	Z
C	0.583022	-0.092353	-0.182265
C	1.632866	0.908892	-0.599670
C	0.074007	2.244026	-0.010186
C	-0.498551	0.880607	0.423085
H	0.221541	-0.691889	-1.040997
H	0.983437	-0.753636	0.615632
H	-1.516876	0.694049	0.020239
H	-0.503019	0.793898	1.526078
C	1.614755	2.025467	0.433776
H	2.263266	2.889339	0.189902
H	1.671750	1.731059	1.500492
C	1.525948	1.533225	-1.853426
H	2.285461	2.333453	-1.982747
C	0.132991	2.189382	-1.623294
H	0.157249	3.193238	-2.095735

Continued on next page

Atom	X	Y	Z
H	-0.775253	1.674328	-2.008535
H	-0.446854	3.120262	0.434818
Si	0.885893	-0.963495	-4.770079
C	1.384588	0.755296	-5.332201
H	1.476963	1.375904	-4.413087
H	0.628568	1.210895	-6.004316
C	-0.814292	-0.951186	-3.969222
H	-1.128967	-1.970781	-3.666163
H	-0.787559	-0.317044	-3.059544
C	2.185372	-1.731375	-3.660213
H	3.158447	-1.828002	-4.184694
H	2.327458	-1.065356	-2.782706
O	2.019933	-0.859213	2.526451
S	1.354218	-0.255341	3.726785
O	0.661103	1.055875	3.480546
O	2.114254	-0.348752	5.002518
C	-0.106904	-1.431488	4.012393
F	0.312072	-2.698180	4.244093
F	-0.930779	-1.472848	2.931229
F	-0.858115	-1.052783	5.074076
H	-1.581875	-0.539198	-4.656369
H	1.883081	-2.734523	-3.296290
H	2.363974	0.750065	-5.853438
F	0.760907	-1.918424	-6.131096

References

[1] Luca McDermott, Zach G Walters, Sarah A French, Allison M Clark, Jiaming Ding, Andrew V Kelleghan, KN Houk, and Neil K Garg. A solution to the anti-bredt olefin synthesis

problem. *Science*, 386(6721):eadq3519, 2024.

[2] Hans Horn and Reinhart Ahlrichs. Fully optimized contracted gaussian basis sets for atoms li to kr. *J. chem. Phys*, 97:2571.

[3] Axel D Becke. Density-functional exchange-energy approximation with correct asymptotic behavior. *Physical review A*, 38(6):3098, 1988.

[4] John P Perdew, Kieron Burke, and Matthias Ernzerhof. Generalized gradient approximation made simple. *Physical review letters*, 77(18):3865, 1996.

[5] Julian Tirado-Rives and William L Jorgensen. Performance of b3lyp density functional methods for a large set of organic molecules. *Journal of chemical theory and computation*, 4(2):297–306, 2008.

[6] Florian Weigend and Reinhart Ahlrichs. Balanced basis sets of split valence, triple zeta valence and quadruple zeta valence quality for h to rn: Design and assessment of accuracy. *Physical Chemistry Chemical Physics*, 7(18):3297–3305, 2005.

[7] Frank Neese. The orca program system. *Wiley Interdisciplinary Reviews: Computational Molecular Science*, 2(1):73–78, 2012.

[8] Frank Neese. Software update: The orca program system—version 6.0. *Wiley Interdisciplinary Reviews: Computational Molecular Science*, 15(2):e70019, 2025.

[9] Stefan Grimme, Stephan Ehrlich, and Lars Goerigk. Effect of the damping function in dispersion corrected density functional theory. *Journal of computational chemistry*, 32(7):1456–1465, 2011.

[10] William Humphrey, Andrew Dalke, and Klaus Schulten. Vmd: visual molecular dynamics. *Journal of molecular graphics*, 14(1):33–38, 1996.

[11] Graeme Henkelman, Blas P Uberuaga, and Hannes Jónsson. A climbing image nudged elastic band method for finding saddle points and minimum energy paths. *The Journal of chemical physics*, 113(22):9901–9904, 2000.

[12] Vilhjálmur Ásgeirsson, Benedikt Orri Birgisson, Ragnar Bjornsson, Ute Becker, Frank Neese, Christoph Riplinger, and Hannes Jónsson. Nudged elastic band method for molec-

ular reactions using energy-weighted springs combined with eigenvector following. *Journal of chemical theory and computation*, 17(8):4929–4945, 2021.

[13] Henry Eyring. The activated complex in chemical reactions. *The Journal of chemical physics*, 3(2):107–115, 1935.

[14] Eric D Glendening and Frank Weinhold. Efficient evaluation of poly-electron populations in natural bond orbital analysis. *Chemical Physics Letters*, 711:23–26, 2018.

[15] Iman Sabeeh Hasan, Alhussein Arkan Majhool, Mustafa Humam Sami, Mohaned Adil, and Saripah Salbiah Syed Abdul Azziz. Dft investigation of structure, stability, nbo charge on titanium—nitrogen nanoheterofullerenes evolved from a small nanocage. *Chemical Review and Letters*, 6(3):297–307, 2023.

[16] ED Glendening and J Badenhoop. K., ae reed, je carpenter, ja bohmann, cm morales, p. karafiloglou, cr landis, f. weinhold. *Theoretical Chemistry Institute, University of Wisconsin, Madison (2018)*, 2018.

[17] Alan E Reed and Frank Weinhold. Natural bond orbital analysis of near-hartree–fock water dimer. *The Journal of chemical physics*, 78(6):4066–4073, 1983.

[18] Alan E Reed, Robert B Weinstock, and Frank Weinhold. Natural population analysis. *The Journal of chemical physics*, 83(2):735–746, 1985.